Effects of Nanomaterials on Drug Coencapsulation and Targeted Drug Delivery

Zhihao Wang

Department of Physical & Environmental Sciences, University of Toronto, Toronto, Canada Corresponding author: aaaron. wang@mail.utoronto.ca

Abstract:

Porous nanocarriers have emerged as versatile platforms for overcoming key limitations of traditional drug delivery systems by enabling precise co-encapsulation of multiple therapeutics and highly selective tumor targeting. This review surveys three major categories of nanocarriers, such as lipid-based, polymeric, and inorganic architectures, and highlights representative strategies such as liposome-inliposome concentrisomes, mesoporous lipid nanoparticles (MLNPs), polymer-gatekeeper hollow silica nanoparticles (PHMSNs), and pH-sensitive gold nanoclusters. The article discuss how co-loading hydrophilic and hydrophobic agents at fixed ratios enhances therapeutic synergy and bypasses multidrug resistance and how surface functionalization or environmental triggers drive tumorspecific accumulation. Key challenges including complex syntheses, high manufacturing costs, immune clearance, premature payload leakage, and regulatory hurdles are examined. Finally, the article outlines current limitations of multi-stage delivery architectures, insufficient deeper tumor penetration, and the absence of robust and scalable production frameworks. By integrating these advances, nanocarriers hold promise for more effective, patientfriendly therapies across oncology and beyond.

Keywords: Nanoparticle; Chemistry; Biology.

1. Introduction

Nanoparticle has been generated for over 30 years, and it has been variously applied in chemistry and biology field. but only recently have biologists begun to exploit their less than 100 nm dimensions and tunable surfaces for advanced drug delivery. Recent research on nanocarriers centers on three main areas: multi drug co-encapsulation, slow release, and targeting.

Traditional carriers typically encapsulate a single

agent, so administering combination regimens requires separate formulations. However, different drugs often have disparate solubilities, stabilities, and pharmacokinetics, which might lead to uncoordinated biodistribution, suboptimal dosing, and will increase toxicity when given as free combinations [1]. Nanocarriers overcome this by co-encapsulating multiple agents at fixed ratios in one particle. For example, polymeric and inorganic nanoparticles synchronously deliver hydrophilic and hydrophobic drugs, boosting therapeutic synergy and improving survival versus

single drug treatments [1]. Additionally, traditional drug delivery system constantly struggled by problem of low accuracy and rapid drug lost which diminishes therapy efficiency substantially and forces patients to consume drug more regularly [2]. Traditional drugs deliveries are unable to selectively release payloads and often releasing drugs before reaches targeted area, while nano carriers that synthesized of pH sensitive or redox sensitive polymers can release drugs own when functional tail react with receptor ends [3]. Current nano targeting strategies already demonstrate measurable gains in organ specific and tumor specific delivery. For example, antibody conjugated nanoparticles achieve about 3 to 5 % percent injected dose per gram (ID/g) in tumors at 24 h [3].

Therefore, based on those current situations, the goal of this review is to summarize main categories and strategies applied in nanocarriers' co-encapsulation and targeting to illustrate how nanocarriers overcome key limitations of traditional drug delivery systems.

2. Drug Co-encapsulation

The multi-drug nanomedicine refers to co-delivering more than one drug to the same site at the same time using a single nanoformulation [1]. The reason why nanoparticle has been chosen is the property of co-encapsulation, indicating that two or more drugs are able to be loaded into the same nanoparticle [1]. It enables drug not only reaching tumer sites at the same time and released to the same cell, but also releasing a controlled ratio [1]. The advantage of multi-drug nanotherapy has been tested. In tumor growth inhibition, the multi-drug nanotherapy reaches further 42.6%, 30% and 29.1% stronger inhibition of tumor growth than single drug free therapy, single drug nanotherapy, and multi-drug free therapy separately [1]. Additionally, triple drug nanotherapy has found to have 6.5% more inhibition of tumor compare to double drug nanotherapy [1]. The usage of nanoparticle forces it to have properties of improving drug stability and solubility, and controlling drug release [1]. There are three main types of nanocarriers being used in therapy currently, lipid, polymeric and inorganic [2].

2.1 Polymeric-Based NP

Polymeric nanoparticles enable the co-encapsulation of hydrophilic and hydrophobic drugs through multiple mechanisms: drugs can be physically localized within the nanoparticle core, entrapped in the polymer matrix, formed covalent bonded to the polymer chains, or adsorbed onto the nanoparticle surface [2]. One of the polymetric based nanocarrier is the MLNP, which is combined by two distinct layers. One layer is poly(bis(4-carboxyphenoxy)phosphazene) (PDCPP), yielded by mixing

heated Hexachloro-cyclotriphosphate and -P-Cl bonds following by reacting with sodium propyl-p-hydroxybenzoate [2]. The other layer is the drug loaded CaCO₃ nanoparticle (CCNPs) [2]. Two distinct dissolved drugs Cisplatin and Chrysin are co-precipitated with CaCl2 and collected by centrifuging and redispersing [2]. Finally, alternating bilayers of cationic CCNPs and anionic PDCPP are deposited using poly(diallyldimethylammonium chloride) (PDADMAC) to assemble the multilayered delivery system [2].

The size of the MLNP land in the range of 200 to 500 nm, which allows them to extravasate and accumulates preferentially in the leaky vasculature of solid tumors. Additionally, the magnitude of zeta potential of MLNP increases with respect to the increasing layer and its charge alters corresponding to each additional layer [4]. Each PDADMAC contribute to negative surface charge and each PDCPP layer derives positive surface charge [2]. Since MLNP is designed to rescue human oral epidermoid carcinoma cell line (KB cells) which covered by a negative charge surface membrane, the cationic MLNPs first adhere to the negatively charged KB cell membrane via electrostatic interactions. They are then internalized through endocytosis and trafficked to perinuclear vesicles, where the acidic microenvironment triggers sustained drug release, positioning the payloads close to the nucleus over time [2]. The alternating of cationic and anionic layer is hydrophilic, allowing liquid flux to take drugs outside. According to experimental data, in the first few hours, about 25% of outmost cisplatin and chrysin in the burst phase are released at pH 5.5 in tumor environment and 15% at pH 7.4 in normal blood environment. After that, the inherent drugs slowly penetrate layers of polymers through liquid flux [2]. Over 80 hours, about 83% of both drugs released at pH 5.5 and 62% of drugs released pH 7.4. The robust PDADMAC-PDCPP shell structure remains its integrity, ensuring controllable release rate [2]. The efficiency of therapy of co-encapsulation is also tested in this material. In one experiment, all MLNP formulations are labeled with the same amount of FITC and incubated with KB cells, and the co-encapsulation of two drugs in MLNPs indicate highest average FICT intensity, indicating the strongest drug delivery potential inside KB cells [2]. Another experiment used to indicate survival of KB cells after injection of three medicines indifferent concentrations in 12 hours and 24 hours respectively indicates that the survival of KB cells co-encapsulation of cisplatin and chrysin in MLNPs is lower than single encapsulation of either cisplatin or chrysinin MLNPs, underscoring outstanding therapy performance of co-encapsulation [2].

2.2 Inorganic-Based NP

Mechanism of co-encapsulation of inorganic nanoparticle

ISSN 2959-6157

such as mesoporous silica utilize changeable pore sizes, surface polarity, PEGylation, and pH-responsive linkers to achieve simultaneous loading and controlled release of diverse therapeutic agents [3]. One of the example is the polymer gratekeeper-hollow mesoporous silica nanoparticles (PHMSNs) [3]. Drug-loaded PHMSNs are prepared by first loading camptothecin into sonicated hollow mesoporous silica nanoparticles and then incubating these CPT-loaded particles with doxorubicin hydrochloride [3]. A PEG-PDS-DPA copolymer shell is then adsorbed and crosslinked via dithiothreitol-induced disulfide cleavage, and the resulting PHMSNs are purified by centrifugation and washing [3].

The tertiary amine unit of PHMSNs become protonated in acidic environment, and the zeta potential of surface charge become positive [3]. PHMSNs permit co-encapsulation by physically adsorbing hydrophobic drugs into the mesoporous silica shell and loading hydrophilic drugs within the hollow core [3]. When the drug loaded PHMSNs enter acidic tumor microenvironment with pH value of 6.5, it surfaces zeta potential become positive and attach to negatively charged tumor membrane by electrostatic interaction [3]. The positive charge causes the PDA unit to swell and extend the size of exterior mesopore, and liquid flux lead hydrophilic drugs to diffuse out quickly. However, the rigid silica pore does not affect by pH change and still hold hydrophobic drugs tightly [3]. When PHMSNs further reaches the cytosol, intracellular glutathione (GSH) or added DTT cleaving pyridyl-disulfide crosslinks in the polymer shell, causing structure cleavage and permitting releasing of hydrophobic drugs [3]. To evaluate co-encapsulation and pH-dependent uptake, KB cells were incubated with drug-loaded PHMSNs for 2 hours at either physiological pH 7.4 or tumor-like pH 6.5, then imaged for the blue CPT and red Dox fluorescence. Figure 1a shows strong blue and red signals and clear co-localization, indicating robust dual-drug internalization. Additionally, Figure 1b and 1c demonstrates poor uptake ability of PHMSN under normal physiological conditions [3]. A pronounced rightward shift at pH 6.5 confirms significantly enhanced drug accumulation [3]. Similarly, the low viability of KB cell in low pH value indicates higher drug accumulation [3]. The therapeutic advantage of co-encapsulation is further demonstrated in vitro [3]. Researchers treat Dox-resistant MCF7/ADR breast cancer cells for 48 hours with either free Dox or Dox-loaded PHMSN at equivalent drug concentrations [3]. Across all doses, the cancer cell viability is consistently lower for the co-encapsulated formulation than for each free Dox, and the difference in cell viability enlarged with increasing concentration [3].

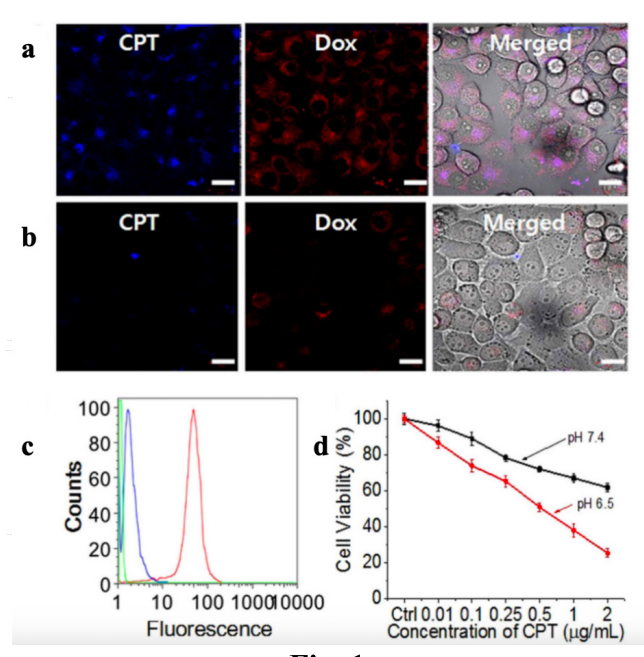


Fig. 1

Fig. 1 (a) and (b) show fluorescence microscopy images of KB cells after a 2 h exposure to dual drug-loaded PHMSNs in DPBS at pH 6.5 and pH 7.4, respectively. (c) presents flow cytometry histograms comparing nanoparticle uptake at pH 7.4 (red), pH 6.5 (blue), and standard culture medium (green) following the same incubation period. (d) illustrates the dose-dependent cytotoxic effects of the dual drug-loaded PHMSNs on KB cells under varying pH conditions [3].

2.3 Lipid-Based NP

The lipid-based NP involved phospholipids with hydrophilic head and hydrophobic tails. it forms unilamellar and multilamellar vesicular structures, and those structures enable hydrophobic drugs stored inside the bilayer membrane and hydrophilic drugs inside the aqueous core. One example of lipid based nanocarrier is the concentrisome. Its liposome in liposome structure engineered by Imperial College London [4]. It is synthesized by microfluidic hydrodynamic focusing (MHF) and the strain-promoted azide-alkyne cycloaddition (SPAAC). The synthesis of the carrier is from the inner liposome formed of DSPE-PEG2K-DBCO covering by the second liposome formed of DSPE-PEG_{2K}-N₃ [4]. The PEG that weighted 2 kilodaltons act as linker to locate two liposome layers [4]. The resulting concentrisomes have a clear nested bilayer morphology, confirmed via cryo-TEM and DLS [4]. Spacing between layers can be adjusted by weight of PEG. For example, PEG_{2K} with PEG_{2K} yields 23 nm, PEG_{2K} with PEG_{5K} yields 34 nm, and PEG_{5K} with PEG_{5K} yields 44 nm [4]. By assigning different temperatures in different layers,

the concentrisomes can release drugs in different layer in order [4]. According to the experiment, the drug releasing process from the outer compartment begins when temperature reaches 42°C, resulting in almost 40% release of outer layer drug [4]. At a higher temperature close to 52°C, about 50% of inner layer drug has been released [4]. Additionally, by changing the size of PEG linkers, the volume of different layer can be manipulated, and the ratio of various drugs can also be controlled [4].

3. Drug Targeting

Nanomedicine targeting is defined to transfer therapeutics selectively to desired sites of action, while slighting interplay with non-targeted tissues and cells [5]. It aims to apply various types of targeting strategies, including cationic lipid-mediated, ligand-mediated, pH-sensitive targeting or magnetic targeting to strengthen accumulation of medicines at desired sites [5].

3.1 Ligand-Mediated Targeting

Ligand-mediated targeting means that nanomedicines are functionalized with tumor-specific ligand that selectively bind receptors and express on target cells [5]. One example is the nanoparticle that composed of PEG-chitosan-lipid micelles and PEG-CS shell (PCL-CP NPs) [6]. PCL-CP NPs are synthesized from PEG-chitosan-lipid (PCL) polymers which composed of chitosan backbone, PEG₂₀₀₀ and lipid chain [6]. Polymers then cover chemothrapy drug to form chemotherapy drug-loaded PCL micelles.[6] Those

micelles are complexed electronically with pre-siRNA in ratio of 10:1 to form drug loaded micelles [6]. Finally, the anionic shell of chondroitin sulfate and PEG-chondroitin is adsorbed onto the micelle surface [6].

The mechanism of targeting is that CS polysaccharides on its outer surface, and CS polysaccharides will react with CD-44 receptors in tumor and deliver drugs into the targeted area [6]. To test targeting performance of PCL-CP NPs, researchers compare radiant efficiencies of free DiR drug and DiR coated by PCL-CP NP in CT26 tumor-bearing mice using 24 h post-intravenous injection under NIRF whole body imaging and ex vivo imaging [6]. The NIRF whole body imaging located in left most diagram in Figure 2 indicates the that the DiR coated by PCL-CP NP are more accumulated in specific area compare to the free one under both DiR filter and Cy5.5 filter [6]. Charts of DiR and Cy5.5 also indicate that the average radiant efficiency of DiR coated by PCL-CP NP has the highest efficiency on targeted tumor, and the second highest efficiency located on liver [6]. Red spots in ex vivo imaging in the middle exhibit high accumulation of DiR drug in tumor as well. Figure 2b examines the performance of PCL-CP on elongate accumulation of drug Dox [6]. By comparing with free Dox, the PCL-CP coated Dox has higher half-life, smaller volume of distribution (Vd) and smaller clearance (CL), the rate of loss of drug [6]. Those data proves that the PCL-CP NP has strong targeting performance and accumulation of drugs in tumers compare to free drugs [6].

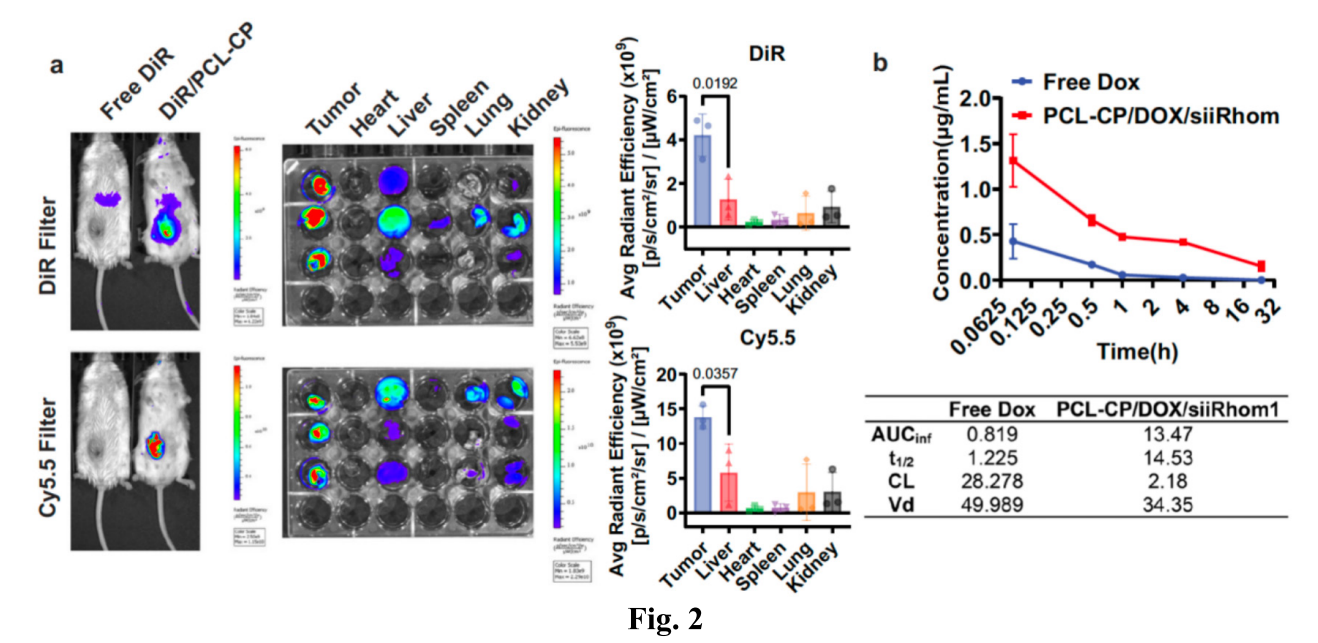


Fig. 2 PCL-CP NPs primarily accumulate in CT26 tumors while exhibiting minimal liver uptake. (a) Near-infrared

fluorescence (NIRF) whole-body and ex vivo images of CT26 tumor-bearing mice 24 h after intravenous injection

ISSN 2959-6157

of DiR-loaded, Cy5.5-labeled PCL-CP NPs (n = 3). (b) Plasma pharmacokinetic profiles comparing free doxorubicin with doxorubicin/siRNA co-loaded PCL-CP NPs following i.v. administration, analyzed by non-compartmental methods to determine AUC₀inf (area under the concentration-time curve), half-life ($t_{1/2}$), clearance (CL), and volume of distribution (Vd) (n = 3) [6].

3.2 Cationic Lipid-Mediated Targeting

Cationic lipid-mediated targeting means electronic interaction of NPs' superficial cationic lipids with the negatively charged cell membranes or extracellular matrix of target cells [1]. The cation degradable lipid CAD-9 is one example of cationic lipid-mediated targeting. It is synthesized in a twostep method, imine formation and imine reduction, using Schiff based reducing methodology [7]. Lipids microfluidically mixed with mRNA and Cholesterol to form CAD lipid nanoparticle (CAD LNP) [7]. The overarching aim of the CAD lipid library is to identify formulations that both efficiently encapsulate mRNA and deliver it to targeted organ [7].

According to Figure 3a, the top 96 lipids that yield the highest luciferase signal were chosen in vivo barcoded

tropism screening [7]. Each candidate LNP was co-encapsulated with a unique DNA barcode, pooled, and injected into mice using six hours post-injection [7]. By comparing barcode-enrichment fold-changes that normalized to the tissue mean, four formulations, CAD3, CAD4, CAD9 and CAD10, are the most organ-selective according to Figure 3b to 3f [7]. Notably, CAD9 drove about 90% of total lung bioluminescence, CAD3 was spleen-biased, and CAD10 preferentially targeted liver [7]. CAD9's apparent pKa is 5.8, lands below the canonical hepatic window, from pH 6.0 to pH 7.0 [7]. It ensures that lipid nanocarrier remains neutral in blood to avoid ApoE-mediated liver uptake and to acquire positive charge in the mildly acidic endosomal compartments of lung cells, which enables attachment to extrahepatic tissues like lung [7]. Each CAD lipid also contains two secondary amine headgroups [7]. During protonation process, these headgroups not only condense the negatively charged mRNA but also interact electrostatically with cell membranes, which facilitate efficient cellular internalization and endosomal release [7]. These two charge-based features together underlie CAD9's exceptional performance in cationic-lipid mediated targeting to the lung [7].

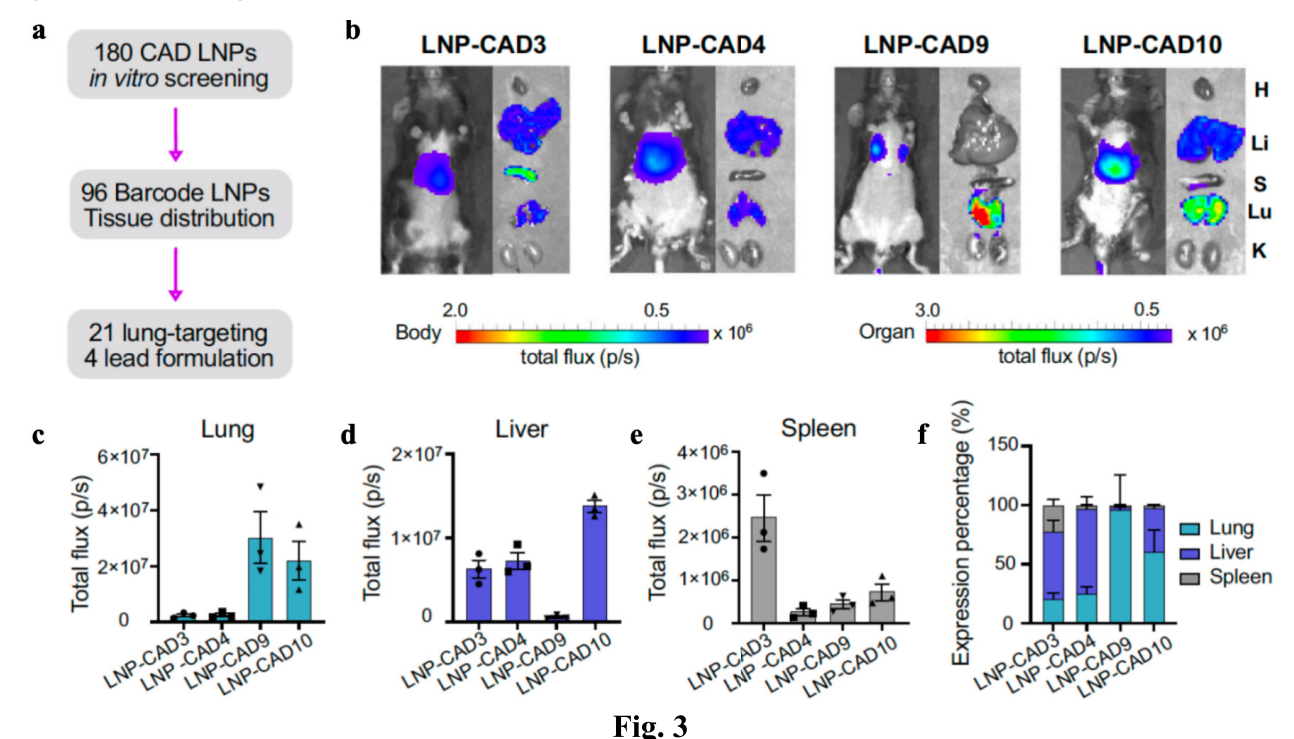


Fig. 3 (a) indicates that four candidate LNP formulations for pulmonary mRNA delivery were identified from a 180-member CAD lipid library via sequential high-throughput in vitro and in vivo screens. (b) indicates that six hours after intravenous administration of 0.1 mg/kg firefly luciferase mRNA encapsulated in LNP-CAD3,

CAD4, CAD9, or CAD10, whole-body and ex vivo imaging revealed organ-specific luciferase expression (H = heart, Li = liver, S = spleen, Lu = lung, K = kidney; n = 3). Quantitative region-of-interest analysis confirmed luciferase activity in the lungs (c), liver (d), and spleen (e), and (f) summarizes the relative expression levels across all

measured organs [7].

3.3 pH-Sensitive Targeting

pH-sensitive targeting means that pH-sensitive lipids in the nanomedicine formulation undergo conformational changes in the acidic tumor microenvironment, triggering drug release [5]. One of the pH sensitive targeting examples is the 6-Aminohexanoyl-glutathione-coated gold nanoclusters (C6A-GSH@AuNCs) [8]. It is the originated from C6A-GSH ligand that synthesized from condensation of N-(2-Aminoethyl) piperidine (C6A) and carboxyl group of glutamic acid in GSH in neutral circumstance [8]. After that, the ligand mixes with HAuCl₄ and add NaOH to neutralize pH value [8]. Finally, after the water bath and purification, the 2nm AuCNs are synthesized [8].

Characters of C6A-GSH@AuCNs are highly sensitive to pH value [8]. The pH value of blood in normal condition is neutral, from 7.2 to 7.4, while the pH value for tumor microenvironment is more acidic, ranges from pH 6.5 to pH 6.8 [8]. In Figure 4a, the diameter of C6A-GSH@AuCNs increases from 2nm in pH 7.4 to about 100nm in

pH 6.5, which magnifies about 50 times.[8] In Figure 4b, the zeta potential of C6A-GSH@AuCNs alters from -8.96 mV to 10.96 mV as the pH value decreases from 7.4 to 6.5 [8]. Its zeta potential almost remains the same absolute magnitude, while opposite sign in certain range of pH [8]. Figure 4c provide the titration curve shows 50 % protonation at pH 6.71, precisely between pH value of blood and tumor [8]. Those three data strongly prove the targeting potential of C6A-GSH@AuCNs because the size of C6A-GSH@AuCNs remains small so that it penetrates tumor interstitium successfully, and its size magnify so that it will be physically locked inside the tumor [8]. Additionally, the shifting point of C6A-GSH@AuCN pH value lands precisely in tumor microenvironment's pH value range [8]. when C6A-GSH@AuCNs enter tumor microenvironment, the zeta potential, which indicate surface charge, becomes positive, and it will be attracted to the negative charge from cancer cell membrane and tumor matrix [8]. As more carriers attach to cell membrane, drug accumulate correspondingly [8].

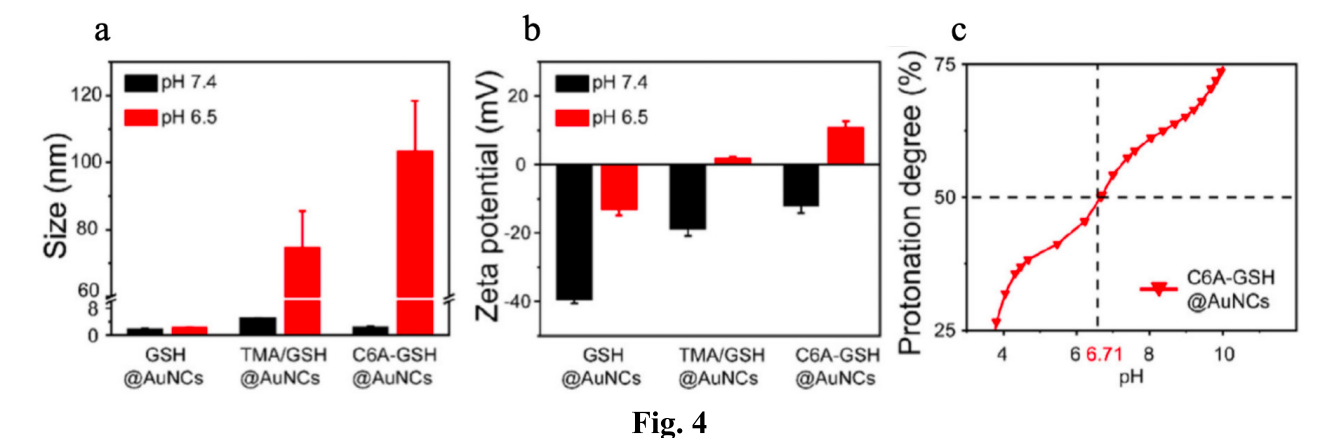


Fig. 4 (a) Comparative hydrodynamic diameters measured by dynamic light scattering at pH 7.4 and pH 6.5. (b) Corresponding zeta potential values indicating surface charge changes between neutral and acidic environments. (c) pH titration curve of C6A-GSH-functionalized AuNCs, demonstrating their buffering capacity across the tested pH range [8].

To measure tumor delivery of C6A-GSH@AuCN, ⁶⁸Ga-labeled AuNCs was injected to 4T1 tumor bearing mice and PET/CT was applied to detect the radioactivity measured in 1 gram of tissue over total amount of drug injected

(%ID/g) as shown in Figure 5a [8]. According to Figure 5e, the red line inclines steeply from about 1.5 %ID/g to 3 %ID/g whereas the other two lines almost remain the same [8]. It indicates that the pH-sensitive targeting C6A-GSH@AuNCs promote strong drug accumulate in tumor, which means strong targeting performance [8]. By comparing Figure 5e with 5b to 5d, the C6A-GSH@AuCN exhibiting constantly low or even decreasing uptake in liver, spleen and kidney, indicating that the C6A-GSH@AuCN achieve both enhanced tumors targeting and reduced off-target deposition compared to other organs [8].

ISSN 2959-6157

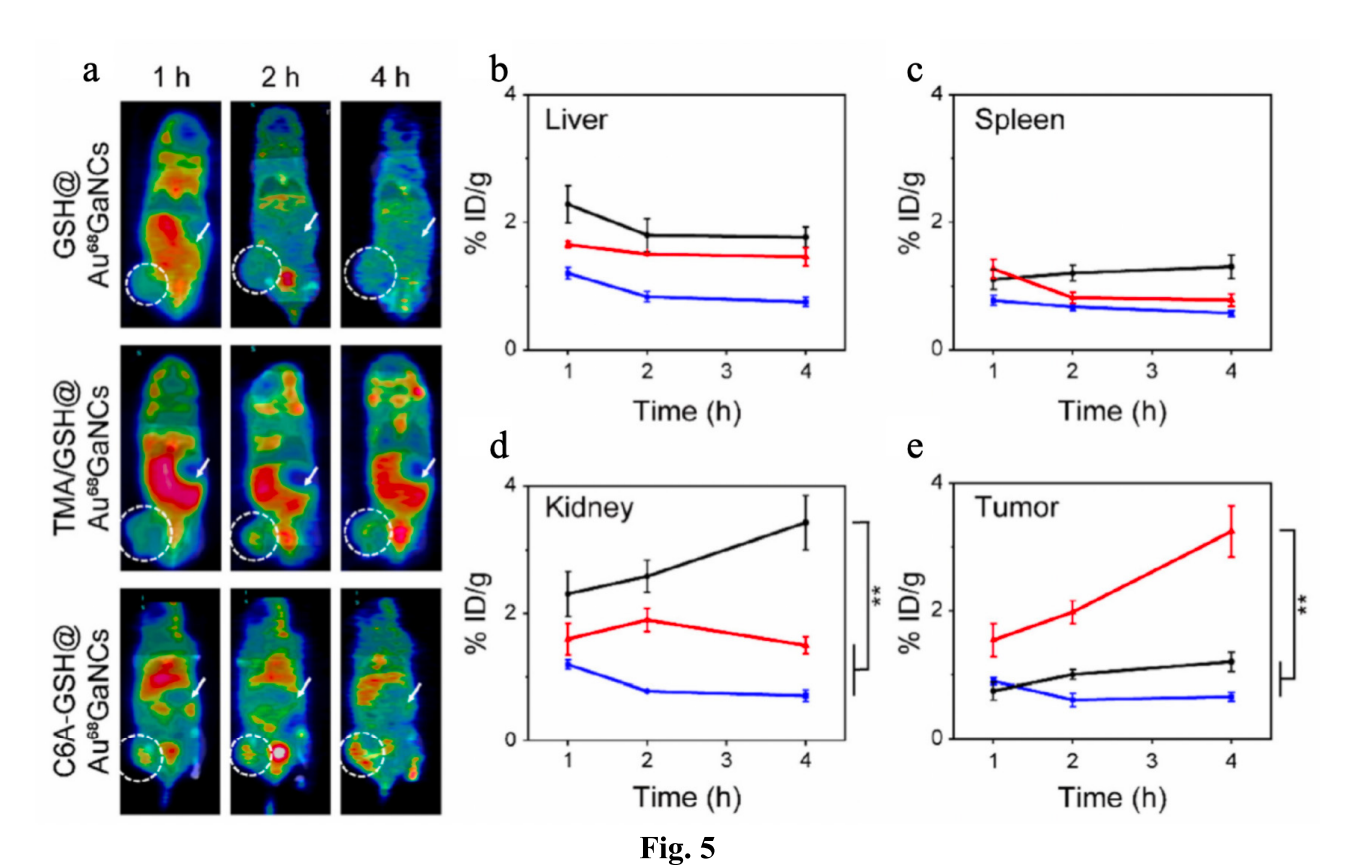


Fig. 5 (a) Representative PET/CT overlays at 1, 2, and 4 h after intravenous administration of ⁶⁸Ga-labeled AuNCs. Circles denote tumor sites; arrows indicate renal uptake. Quantitative ROI analysis of time-dependent radiotracer accumulation in (b) liver, (c) spleen, (d) kidney, and (e) tumor over 4 h post-injection. Data are shown for GSH@ Au⁶⁸GaNCs (blue), TMA/GSH@Au⁶⁸GaNCs (black), and C6A-GSH@Au⁶⁸GaNCs (red); *P < 0.05, **P < 0.01 [8].

4. Limitations

Nanocarriers encounter several challenges. For example, their poor penetration into hypoxic, fibrotic tumor cores limits its uniformity of drug distribution [1]. Additionally, even PEGylated nanocarriers undergo opsonization and accelerated blood clearance, which shortens their circulation time and increases the risk of off-target toxicity [3]. Moreover, the elaborate, long term and massive step syntheses not only challenge nanocarriers' reproducibility under GMP but also drive up production costs, which makes clinical translation and market pricing prohibitive [4]. What's more, premature payload leakage and incomplete, non-synchronous release at the tumor site further compromise therapeutic efficacy, and the need for distinct safety and efficacy studies for each functional component of multiplexed or theranostic platforms creates additional regulatory roadblocks [1, 3].

5. Conclusion

Nanocarriers represent a transformative advance over conventional dosage forms by integrating co-encapsulation and targeting into unified, nanoscale constructs. Lipid-based systems such as concentrisomes demonstrate programmable, temperature-layered release, while polymeric nanoparticles coordinate hydrophilic and hydrophobic payloads through pH- and redox-responsive mechanisms to overcome drug resistance in vitro. Across these classes, stimuli-responsive gating and ligand conjugation have increased tumor accumulation in preclinical models. However, multifaceted challenges persist: elaborate, multi-step syntheses hinder reproducibility and scale-up; PEGylation reduces but does not eliminate opsonization and rapid clearance; premature leakage and incomplete, non-synchronous release compromise efficacy; and multiplexed or theranostic constructs face complex regulatory pathways. With continued integration of computational design and manufacturing innovations, nanocarriers will be poised to transition from proof-of-concept studies to clinically viable, precision therapeutics.

References

[1] Benderski, K., Lammers, T. & Sofias, A.M. Analysis of multi-drug cancer nanomedicine. Nat. Nanotechnol., 2025, 20,

ZHIHAO WANG

7165.

- [2] Mehnath, S.; Mukherjee, A.; Rajan, M.; et al. Co-Encapsulation of Dual Drug Loaded in MLNPs: Implication on Sustained Drug Release and Effectively Inducing Apoptosis in Oral Carcinoma Cells. Biomed. Pharmacother, 2018, 104, 661–671.
- [3] Palanikumar, L.; Jeena, M. T.; Kim, K.; et al. Spatiotemporally and Sequentially-Controlled Drug Release from Polymer Gatekeeper-Hollow Silica Nanoparticles. Sci. Rep., 2017, 7, 46540.
- [4] Pilkington, C.P., Gispert, I., Chui, S.Y. et al. Engineering a nanoscale liposome-in-liposome for in situ biochemical synthesis and multi-stage release. Nat. Chem., 2024, 16, 1612–1620.
- [5] Tekade, R. K.; Maheshwari, R.; Tekade, M.; Chougule, M. B. Solid Lipid Nanoparticles for Targeting and Delivery of Drugs

- and Genes. Nanotechnology-Based Approaches for Targeting and Delivery of Drugs and Genes, 2017, 8, 256-286.
- [6] Luo, Z.; Huang, Y.; Batra, N.; Chen, Y.; et al. Inhibition of iRhom1 by CD44-Targeting Nanocarrier for Improved Cancer Immunochemotherapy. Nat. Commun., 2024, 15, 255.
- [7] Xue, L.; Hamilton, A. G.; Zhao, G.; Xiao, Z.; et al. High-Throughput Barcoding of Nanoparticles Identifies Cationic, Degradable Lipid-Like Materials for mRNA Delivery to the Lungs in Female Preclinical Models. Nat. Commun., 2024, 15, 1884.
- [8] Jiang, Y.; Wu, Q.; Hou, M.; et al. pH-Sensitive Gold Nanoclusters Labeling with Radiometallic Nuclides for Diagnosis and Treatment of Tumor. Mater. Today Bio., 2023, 19, 100578.